



## OPEN ACCESS

## EDITED BY

Zhi-Qiang Jiang,  
East China University of Science and  
Technology, China

## REVIEWED BY

Jan Korbelt,  
Medical University of Vienna, Austria  
Yin-Jie Ma,  
East China University of Science and  
Technology, China  
Xin Zhang,  
Shanghai Maritime University, China

## \*CORRESPONDENCE

Lu Qiu,  
nuaaqiulu@shnu.edu.cn

## SPECIALTY SECTION

This article was submitted to Social  
Physics,  
a section of the journal  
Frontiers in Physics

RECEIVED 20 September 2022

ACCEPTED 24 October 2022

PUBLISHED 09 November 2022

## CITATION

Qiu L, Su R and Wang Z (2022), Financial  
crisis prediction based on multilayer  
supervised network analysis.  
*Front. Phys.* 10:1048934.  
doi: 10.3389/fphy.2022.1048934

## COPYRIGHT

© 2022 Qiu, Su and Wang. This is an  
open-access article distributed under  
the terms of the [Creative Commons  
Attribution License \(CC BY\)](https://creativecommons.org/licenses/by/4.0/). The use,  
distribution or reproduction in other  
forums is permitted, provided the  
original author(s) and the copyright  
owner(s) are credited and that the  
original publication in this journal is  
cited, in accordance with accepted  
academic practice. No use, distribution  
or reproduction is permitted which does  
not comply with these terms.

# Financial crisis prediction based on multilayer supervised network analysis

Lu Qiu<sup>1,2\*</sup>, Rongpei Su<sup>1</sup> and Zhouwei Wang<sup>1</sup>

<sup>1</sup>School of Finance and Business, Shanghai Normal University, Shanghai, China, <sup>2</sup>Department of Finance, East China University of Science and Technology, Shanghai, China

Financial crisis prediction is essential in preventing financial problems as its monitoring indicators help regulators judge the probability of future crises. In this context, the activities of the scientific community have been focused on the dynamics of single/multiple sequences and utilized unsupervised/supervised methods for financial crisis prediction. It is noteworthy that the cross-correlation between the risks of multiple economic entities makes financial network analysis paramount in crisis prediction. Focusing on this point, we propose a multilayer supervised network analysis (MSNA) method to train the multilayer network, and select the most suitable layer for financial crisis prediction. Specifically, we use 37 crucial stock market indices from 4 continents to create successive multilayer financial networks with 120-day windows and 1-day step by Pearson cross-correlation (PCC), variance decompositions (VD), transfer entropy (TE), minimum spanning tree (MST), directed MST (DMST), planar maximally filtered graph (PMFG) and directed PMFG (DPMFG) methods. Based on the multilayer network, we embed the graph neural network classification (GNNC) model and train the dynamic multilayer networks at each window scale (240, 120, and 60 days). Finally, we conclude that the accuracy of the short window (60 days) is significantly higher than that of the long window. The network constructed by PCC with MST is the most suitable for short sequence (60 days) crisis prediction (AUC = 0.959), and the network constructed by TE with DMST is the most suitable for long sequence (240 days) crisis prediction (AUC = 0.772).

## KEYWORDS

financial crisis prediction, multilayer network, transfer entropy, variance decompositions, graph neural network PACS numbers

## 1 Introduction

A financial crisis refers to various situations, such as stock market crashes and bursting of financial bubbles, in which some financial assets suddenly lose a large part of their nominal value. Many economists have proposed theories about how financial crises develop and how they can be prevented. Frankel and Rose predicted the probability of crises by establishing the joint probability distribution between independent and dependent variables [1]. Subsequently, Kaminsky et al. used the KLR signal analysis method to detect the index signals exceeding the threshold at a certain time point or

period, and used signal strength for crisis prediction [2]. Further, Berg et al. integrated the advantages of the FR probability model and KLR signal analysis method and created DCSD (developing country studies division) model, that can send out early warning signals for crises more accurately and shorten the prediction interval to 24 months [3]. However, the probability model, the KLR signal analysis method and DCSD model do not consider the heterogeneity of the financial crisis and the difference in the actual situation between countries. Sachs et al. constructed an STV cross-sectional model of a currency crisis early warning system based on cross-sectional data [4].

Some scholars have constructed quantitative indices for financial crisis prediction. Billio et al. used an entropy measure to analyze the evolution of systemic risk among European banks and constructed a banking crisis early warning index system based on marginal expected shortfall (MES), conditional value at risk (CoVaR) indicators and network connectivity. Additionally, they determine the effectiveness of entropy measures in banking crisis prediction [5]. Dastkha et al. used CoVaR as a market-based systematic risk measurement method to investigate the systematic risk of the Tehran stock exchange and provide early warning signals of systematic risk [6].

As the FR probability model, KLR signal, and risk quantitative index can only explain the occurrence of crisis and cannot compare and test the early-warning results, Kumar et al. established a logit model to test the effects of early crisis warnings [7]. Moreover, Klomp used a random coefficient logit model to improve the traditional logit model and analyzed the heterogeneity of banking crises from 1970 to 2007 [8]. Schularick et al. used a logit model for crisis prediction and proved that credit growth is a powerful predictor of financial crisis [9]. Similarly, Greenwood et al. posited that crises can be predicted using past credit growth in simple linear forecasting regressions, and that the probability of a financial crisis within the next 3 years is 45% [10]. Boonman et al. applied the KLR Signal method and logit model method to the data of 15 groups of emerging economies, and found that the index prediction based on consistent expectation tended to eliminate extreme situations, resulting in no timely warning when predicting a large number of crises [11]. This shows that the logit prediction model can determine the key leading indicators of the financial crisis. Moreover, some important indicators lead to false early warnings. Simultaneously, the prediction time of the logit model for a crisis remains at 24 months.

To enhance the prediction accuracy of limited data, Sornette et al. used the log-periodic power law singularity (LPPLS) method to evaluate data on the Shanghai and Shenzhen stock indices from May 2005 to July 2009. The results show that the LPPLS method can successfully find the prediction signals before the two-stage sharp decline in China's stock market (from mid-2005 to October 2007, and from November 2008 to early August 2009), and improve the prediction accuracy to approximately

2 months [12]. Fricke used a machine learning model and a traditional logit model to predict various financial crises and discovered that the prediction results of the machine learning model were not always more accurate than those of the traditional logit model [13]. Tölö used long-term and short-term memory (RNN-LSTM) and gated recursive unit (GRU) neural network model for crisis prediction. They found that the prediction effect of the RNN-LSTM method was significantly higher than that of the traditional logit model [14]. Zhu et al. used a K-means clustering algorithm to classify financial risk types and optimize the financial risk control. They found that the K-means algorithm can distinguish the state intervals of different financial crises more accurately and objectively [15]. Liu et al. found that the machine learning models, especially the random forest, gradient boosting decision tree, and ensemble models, outperform logistic models in terms of providing early predictions of financial crises [16].

Nevertheless, LPPLS method and machine learning model generally utilize a single stock for prediction, lack consideration of the correlation analysis between multiple financial institutions, and can not investigate the risk contagion of financial institutions. The question that needs to be considered is as follows: How can the correlation of financial markets be applied to crisis prediction and improve supervised characteristics?

Due to the complexity of the financial system and the unrealistic theoretical assumptions, it is difficult to provide scientific and effective suggestions for economic policies after the financial crisis, and to point out the need to studying financial problems from the perspective of a complex system [17–20]. As an emerging technical means, the financial complex network is very intuitive in describing the relationship of various financial elements. Building an effective financial network has always been the focus of scholars' researchers worldwide. In recent years, many methods have been used to build a financial network. Researchers have used Pearson cross-correlation [21], mutual information [22], Granger causality tests [23, 24], transfer entropy [25] and variance decomposition [26] to create financial matrices expressing the relationship between financial institutions. Additionally, they have used the threshold method [27], MST method [28, 29], plane maximum filter graph method [30], DMST [31] and DPMFG [32] to create financial networks. However, a problem that still needs to be considered is how to build a network that is suitable for financial crisis prediction. Hence, it is necessary to use the crisis prediction results as a supervised condition for the supervision and early warning analysis of high-dimensional financial networks.

Traditional machine learning and neural network models [33–36] have limitations when processing non-Euclidean spatial data (e.g., financial networks, social networks and information networks). In addition, compared with the most basic network structure of neural network containing the total connection layer

(MLP), the graph neural network [37, 38] has an adjacency matrix, which simplifies the calculation form and improves the calculation efficiency.

With the help of the excellent performance of graph neural network method in graph classification, we integrate multilayer network construction method and graph neural network supervised analysis to study the supervision and prediction of financial crisis. The method derived from this paper is called multi-layer supervised network analysis (MSNA). Specifically, we constructed multilayer networks by utilizing PCC, VD and TE combining with MST and PMFG. We employed the graph neural network classification method to add the supervised characteristics to the multilayer networks, and use the existing crises as the tag values to study the supervision and financial crisis prediction.

The remainder of this paper is organized as follows. In Section 2, we present our method (i.e.,MSNA) of the article in two parts: 1) the construction of the multiplex network and, 2) the supervised characteristics of dynamic multiplex networks. In Section 3, our datasets are briefly presented. In Section 4, we show the main results. The findings show that the MSNA model has better prediction results, compared with long series. Second, the first-layer network (PCC-MST) is the most suitable for financial crisis prediction. Section 5 presents the conclusions and discussion.

## 2 Materials and methods

### 2.1 Multiplex network creation

#### 2.1.1 Creating a pearson correlation-coefficient network

The complex relationships between stocks vary with the stock market and the economic environment. Thus we can use these relationships to describe the state of the stock market. We consider many stock log-return series, and each index is as follows:

$$P = \begin{Bmatrix} P_{1,1} & P_{1,2} & \cdots & P_{1,T+1} \\ P_{2,1} & \ddots & \cdots & P_{2,T+1} \\ \vdots & \vdots & \ddots & \vdots \\ P_{M,1} & P_{M,2} & \cdots & P_{M,T+1} \end{Bmatrix} \quad (1)$$

where  $P_{i,t}$  is the price of the index  $i$  on day  $t$ . We calculate the daily return for each index  $i$  as:

$$R = \{r_{i,t+1} \equiv \ln P_{i,t+1} - \ln P_{i,t}, i = 1, 2, \dots, M; t = 1, 2, \dots, T\} \quad (2)$$

where  $T$  denotes the total length of the stock log-return series,  $M$  indicates the number of the log-return series. A series of sequence fragments is extracted from the sequences  $R$  by a sliding window whose length is  $L$ .

$$R_s = \begin{Bmatrix} r_{1,\Delta \bullet (s-1)+1} & r_{1,\Delta \bullet (s-1)+2} & \cdots & r_{1,\Delta \bullet (s-1)+L} \\ r_{2,\Delta \bullet (s-1)+1} & \ddots & \cdots & r_{2,\Delta \bullet (s-1)+L} \\ \vdots & \vdots & \ddots & \vdots \\ r_{M,\Delta \bullet (s-1)+1} & r_{M,\Delta \bullet (s-1)+2} & \cdots & r_{M,\Delta \bullet (s-1)+L} \end{Bmatrix}, \quad (3)$$

$$s = 1, 2, \dots, W, W = \left\lceil \frac{T-L}{\Delta} \right\rceil + 1$$

where  $\Delta$  denotes the sliding step and  $W$  indicates the total number of fragments,  $\lceil \cdot \rceil$  means rounding. The  $s$ th segment of  $R$ ,  $R_s$ , and Pearson correlations between stocks are as follows:

$$\rho_{i,j}(s) = \frac{\sum_{t=1}^L (r_{i,\Delta \bullet (s-1)+t} - \overline{R_s(i, \cdot)}) (r_{j,\Delta \bullet (s-1)+t} - \overline{R_s(j, \cdot)})}{\sqrt{\sum_{t=1}^L (r_{i,\Delta \bullet (s-1)+t} - \overline{R_s(i, \cdot)})^2} \cdot \sqrt{\sum_{t=1}^L (r_{j,\Delta \bullet (s-1)+t} - \overline{R_s(j, \cdot)})^2}}, \quad (4)$$

$$s = 1, 2, \dots, W, i = 1, 2, \dots, M, j = 1, 2, \dots, M.$$

where Eq. 4 represents the correlation coefficient of two sequences of the  $s$  fragments, while  $\overline{R_{s,i}}$  and  $\overline{R_{s,j}}$  represents the average value of the  $i$  row and  $j$  row in formula Eq. 3 respectively.

For these Pearson correlation matrices, we choose two popular methods (MST and PMFG) to create financial networks. The steps of the Kruskal MST method are as follows:

- 1) Translate the Pearson correlation matrix to a distance matrix:

$$D_{ij} = \sqrt{2(1 - \rho_{ij})} \quad (5)$$

where  $D_{ij}$  indicates the distance between stock  $i$  and stock  $j$ ,

- 2) Sort the values from the distance matrix named  $D_{ij}^{ac}$  in ascending order.
- 3) Add the edge to the spanning tree from  $D_{ij}^{ac}$  in ascending order. If the adding edge forms a ring, we select the next value in  $D_{ij}^{ac}$  and skip this edge.
- 4) Repeat step 3 until the number of edges is  $M - 1$ .

The simplest structure can be obtained from the MST, but some important information is ignored. Thus we also use the PMFG method to create a network using a Pearson correlation matrix. The steps of the PMFG method are as follows:

- 1) The correlation degree between each node is arranged in ascending order according to the values in the matrix.
- 2) The corresponding node pairs are selected from the arranged weight values in order to establish the edge connection. If the newly added edge makes the network appear non-planar, that is, if the newly added edge and its other edges cross on a plane, the connection will be abandoned.
- 3) Repeat step 2 until all nodes join the network.

In this way, we constructed the dynamic Pearson correlation matrices into multilayer networks using the MST and PMFG

method. The two networks are regarded as first-layer (PCC-MST) and second-layer (PCC-PMFG) networks.

### 2.1.2 Construction of a risk spillover network

Although the Pearson correlation network can analyze the volatility correlation between stocks, it can not explain the risk spillover between stocks. Therefore, we intend to use the VD method to create a risk spillover network. The steps of the VD method [26] are as follows:

- 1) We construct A VAR(Q) process (1) model based on the relevant infectious variables of financial institutions to establish inter-agency relationships as follows:

$$z_t = \sum_{q=1}^Q \phi_q z_{t-q} + \varepsilon_t \tag{6}$$

$$z_t = \sum_{q=0}^{\infty} A_q \varepsilon_{t-q} \tag{7}$$

where  $z_t$  is a  $M$ -dimensional vector of endogenous variables.  $A_q$  is a  $M$ -by- $M$  matrix,  $\phi$  represents the parameter matrix,  $\varepsilon$  indicates independent and identically distributed perturbed term and follows:  $\varepsilon \sim (0, \Sigma)$ . The forms of  $A_q$  in Eq. 7 are as follows:

$$A_q = \phi_1 A_{q-1} + \phi_2 A_{q-2} + \dots + \phi_p A_{q-p} \tag{8}$$

where  $A_0$  is a unit matrix and  $A_0 = 0$  when  $q < 0$ .

- 2) Based on Eqs 6–8, we obtain the directed correlation coefficients between mechanisms in different periods (forward  $H$  step) using the generalized variance decomposition technique. The calculation formulas are as follows:

$$d_{ij}^h = \frac{\sigma_{ii}^{-1} \sum_{h=0}^{H-1} (e'_i A_h \Sigma e_j)^2}{\sum_{h=0}^{H-1} (e'_i A_h \Sigma A'_h e_i)^2} \tag{9}$$

where  $\Sigma$  is the covariance matrix of the error  $\varepsilon$ ,  $\sigma_{ii}$  is the standard deviation of error for the  $i$ th equation. Further,  $e_j$  is a selection vector with  $j$ th element unity and zeros elsewhere. Additionally,  $d_{ij}^h$  is called directed spillover index of  $j$  over  $i$ . Lastly,  $H$  indicates the number of steps to forward the predicted variance.

The risk spillover network created directly by the directed spillover matrix contains many noise edges. We intend to use DMST and DPMFG to reduce the noise and create multilayer financial networks namely, third-layer (VD-DMST) and fourth-layer (VD-DPMFG) networks. The steps of DMST [39] are as follows:

- 1) Select a node as the root node randomly.
- 2) Travel all edges and find the smallest entry edges of all points except for the root node. Then, the weighted values

of the edges are summed to form a new graph. The final minimum arborescence is determined if no cycles exist in the new graph.

- 3) If a ring exists in the new graph, it shrinks the ring into a point and change the edge weight. The steps to change the edge weights are as follows:

① Choose a node  $u$  in the ring and set the incoming edge of this node as  $in[u]$ , and the outgoing edge of this node as  $(u, i, w)$ . Further,  $i$  and  $w$  refer to the source node and the weight, respectively. ② Set the new edge weight of node  $u$  as  $(u, i, w - in[u])$ . ③ Return to Step 2 if the new weight graph contains rings.

- 4) Expand the new graph if rings do not exist by the breaking loop method [40]. The steps of the breaking loop method are as follows:

① Find a loop in the graph. ② Remove the edge with the largest weight in the loop, but keep the graph connected. ③ Repeat this process until there are no loops in the graph (but they are still connected) and get the minimum spanning tree.

The steps of DPMFG [32] are as follows:

- 1) We convert the asymmetric matrix into a symmetric matrix by summing two edges.
- 2) We use PMFG to transfer the symmetric matrix into a PMFG matrix.
- 3) Based on the result of the PMFG matrix, we select the larger of the two edges to represent the direction and delete the smaller one.

### 2.1.3 Constructing information transmission networks

The risk spillover network can describe the contagion from one stock to others, but cannot describe the co-movement between stocks. Thus we select transfer entropy to express the co-movement and information transmission between stocks. Transfer entropy [41] developed by Schreiber is a measure to evaluate dynamic, nonlinear, and non-symmetric relationships. The measurement of Transfer Entropy is Shannon Entropy. Shannon Entropy is defined as follows:

$$E = - \sum_{t=1}^N p_t \log p_t, \tag{10}$$

for a sequence  $x$  and  $p_t \neq 0$ , where  $N$  is the number of bins by dividing the sequence  $x$ ,  $p_t$  is the probability of the  $t$ th bin by the probability density function (PDF). Based on Shannon entropy, transfer entropy can be conceived as a parameter that can be used for describing the interaction between the series  $X$  and  $Y$ . Reciprocities have directivity,  $TE_{x \rightarrow y}$  or  $TE_{y \rightarrow x}$ . The transition probabilities can be defined as follows:

$$p(x_{t+1} | x_t^{(k)}, y_t^{(l)}) = p(X_{t+1} = x_{t+1} | X_t^{(k)} = x_t^{(k)}, Y_t^{(l)} = y_t^{(l)}) \tag{11}$$

where time series of  $X$  could be treated as a Markov process of degree  $k$ . Likewise,  $Y$  is  $l$  degree Markov process.  $X_t^{(k)} = (X_t, X_{t-1}, \dots, X_{t-k+1})$  and  $Y_t^{(l)} = (Y_t, Y_{t-1}, \dots, Y_{t-l+1})$ .  $x_t^{(k)}$  and  $y_t^{(l)}$  are the states of  $X_t^{(k)}$  and  $Y_t^{(l)}$ , respectively. The transfer entropy from one variable  $Y$  to the other variable  $X$  is defined as follows:

$$\begin{aligned} TE_{Y \rightarrow X}(k, l) &= E(X_{t+1} | X_t^{(k)}) - E(X_{t+1} | X_t^{(k)}, Y_t^{(l)}) \\ &= \sum p(x_{t+1}, x_t^{(k)}, y_t^{(l)}) \log \frac{p(x_{t+1} | x_t^{(k)}, y_t^{(l)})}{p(x_{t+1} | x_t^{(k)})} \\ &= \sum_{i_{t+1}, i_t^{(k)}, j_t^{(l)}} p(i_{t+1}, i_t^{(k)}, j_t^{(l)}) \log \frac{p(i_{t+1}, i_t^{(k)}, j_t^{(l)}) p(i_t^{(k)})}{p(i_{t+1}, i_t^{(k)}) p(i_t^{(k)}, j_t^{(l)})} \end{aligned} \tag{12}$$

where  $i_t$  is element  $t$  of the time series of variable  $X$  and  $j_t$  is element  $t$  of the time series of variable  $Y$ . To facilitate the calculation of transfer entropy, we take  $k = l = 1$ . Thus the normal formula for transfer entropy of stock  $j$  to stock  $i$  is:

$$TE_{j \rightarrow i} = \sum_{i_{t+1}, i_t, j_t} p(i_{t+1}, i_t, j_t) \log \frac{p(i_{t+1}, i_t, j_t) p(i_t)}{p(i_{t+1}, i_t) p(i_t, j_t)} \tag{13}$$

In order to convert transfer entropy matrices into multilayer financial networks. We also use DMST and DPMFG to reduce the noise and create multilayer financial networks, namely, the fifth-layer (TE-DMST) and sixth-layer (TE-DPMFG) networks.

### 2.1.4 Calculation method of multilayer network topology parameters

After implementing the aforementioned methods and conducting a comprehensive analysis, we can obtain the six-layer (comprising PCC-MST, PCC-PMFG, VD-DMST, VD-PMFG, TE-DMST and TE-DPMFG) financial networks. To discover the topological changes of six-layer networks, we use the out-degree, in-degree, PageRank and Hub of single-layer and multilayer networks. The single-layer forms of degree, and out-degree, in-degree are shown in Eqs 14–16:

$$K_i^{[\alpha]} = \sum_{j \neq i} W_{ij}^{[\alpha]} \tag{14}$$

$$K_{i-in}^{[\alpha]} = \sum_i^M W_{ji}^\alpha \tag{15}$$

$$K_{i-out}^{[\alpha]} = \sum_i^M W_{ij}^\alpha \tag{16}$$

where  $W_{ij}^{[\alpha]}$  is an element from a  $(M \times M)$  matrix in  $\alpha$ -layer,  $i = 1, 2, 3, \dots, M, j = 1, 2, 3, \dots, M$ . The PageRank  $PR_i$  of single-layer network with  $M$  nodes is as follows:

$$PR_i^{[\alpha]} = \lambda_t \sum_j^M I_{ij} \frac{PR_j^{[\alpha]}}{g_j^{out}} + (1 - \lambda_t) \frac{1}{M} \tag{17}$$

where  $I_{ij}$  are the elements of the adjacency matrix that are equal to one if node  $j$  points to node  $i$  and zero otherwise. Further,

$g_j^{out} = \max(1, K_j^{out})$  and  $\lambda_t > 0$  are the damping factor. We also use Hub  $HU$  of a single-layer with  $M$  nodes to reflect the role of nodes in information dissemination as follows:

$$HU_i^{[\alpha]} = \sum_{j=1}^M I_{ji} AU_j^{[\alpha]} \tag{18}$$

where  $AU_j^{[\alpha]}$  is the authority of the node  $j$  in the  $\alpha$  layer. These parameters of the multilayer network are illustrated in Eqs 19–23. The degree, in-degree and out-degree [42, 43] of the multilayer network are defined as follows:

$$O_i = \sum_{\alpha=1}^{\theta} K_i^{[\alpha]} \tag{19}$$

$$O_{i-in} = \sum_{\alpha=1}^{\theta} K_{i-in}^{[\alpha]} \tag{20}$$

$$O_{i-out} = \sum_{\alpha=1}^{\theta} K_{i-out}^{[\alpha]} \tag{21}$$

where  $\alpha$  means the layer number,  $\theta$  indicates the total amount of layers. The iterative form of PageRank [44] for a multilayer network is as follows:

$$PR_i^{mul} = \lambda T_{j\beta}^{i\alpha} + \frac{1 - \lambda}{M\theta} u_{j\beta}^{i\alpha} \tag{22}$$

where  $T_{j\beta}^{i\alpha}$  denote the tensor of the transition probabilities for jumping between pairs of nodes and switching between pairs of layers,  $\beta = 1, 2, \dots, 6, \alpha = 1, 2, \dots, 6, i = 1, 2, 3, \dots, M, j = 1, 2, 3, \dots, M$ . Moreover,  $\lambda$  means the walker jumps to a neighbor with rate  $\lambda$  and teleport to any other node in the network with rate  $1 - \lambda$ , while  $u_{j\beta}^{i\alpha}$  is the rank-4 tensor with all components equal to 1. The Hub [45] of multilayer are as follows:

$$HU_i^{mul} = HU_i^{[\alpha]} u^\alpha \tag{23}$$

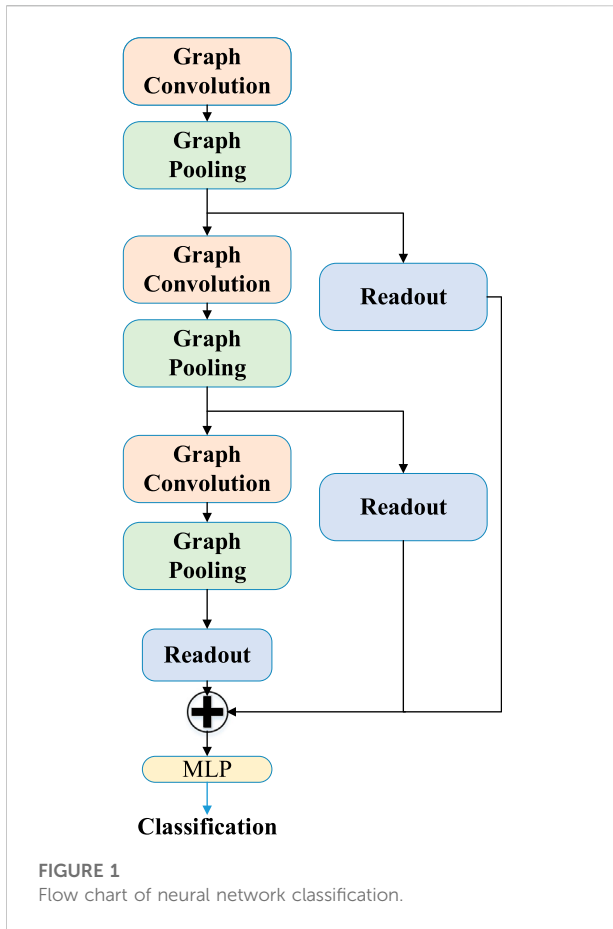
where  $u^\alpha$  represents the rank-2 tensor whose all components equal to 1.

## 2.2 Multilayer supervised network model

### 2.2.1 Graph neural network classification model

Through the foregoing analysis, we can create six-layer networks and obtain their parameters (degree, out-/in-degree, PageRank, Hub). To add the supervision to the six-layer networks, we use the Self-Attention Graph Pooling (SAGPOOL) method [46] (a verified method for graph neural network classification) to train the six-layer networks and find the optimal layer. The detailed steps of the SAGPOOL method are as follows:

- 1) Transform the adjacency matrix data of the six-layer network into a graph neural network classification module.



2) The importance of each node is adaptively learned from the graph using Kipf's concept of graph convolution [47]. The graph convolution formula is as follows:

$$Z = \sigma \tilde{G}^{-\frac{1}{2}} \tilde{W} \tilde{G}^{-\frac{1}{2}} F \Theta_{att} \quad (24)$$

where  $\sigma$  is the activation function (e.g. tanh),  $Z$  is the self-attention score,  $\tilde{W} \in \mathbb{R}^{M \times M}$  is the adjacency matrix with self-connections,  $\tilde{G} \in \mathbb{R}^{M \times M}$  is the degree matrix of  $\tilde{W}$ ,  $F$  is the input features of the graph with  $M$  nodes and  $\theta$ -dimensional features,  $\Theta_{att} \in \mathbb{R}^{\theta \times 1}$  is the only parameter of the SAGPOOL layer.

3) Adopt the node selection method in gpool and retain some nodes of the input graph. The pooling ratio  $\omega \in (0, 1)$  is a hyperparameter that determines the number of nodes to be maintained. The top  $[\omega M]$  nodes are selected based on the value of  $Z$ .

$$idx = top - rank(Z, [\omega M]), Z_{mask} = Z_{idx} \quad (25)$$

where top-rank is the function that returns the indices of the top  $[\omega M]$  values,  $idx$  is an indexing operation and  $Z_{mask}$  is the feature attention mask.

4) Select the TOP  $\omega$  of features and structures according to  $idx$  as follows:

$$F' = F_{idx}, F_{out} = F' \odot Z_{mask}, W_{out} = W_{idx,idx} \quad (26)$$

where  $F_{idx}$  is the row-wise (i.e. node-wise) indexed feature matrix,  $\odot$  is the broadcasted elementwise product, and  $W_{idx,idx}$  is the row-wise and col-wise indexed adjacency matrices. Further,  $F_{out}$  and  $W_{out}$  are the new feature matrix and the corresponding adjacency matrix, respectively.

5) Add a readout layer according to the idea of JK net architecture [48], which aggregates node features to form a fixed size representation:

$$sag = \frac{1}{M} \sum_{i=1}^M w_i \parallel \max_{i=1}^M w_i \quad (27)$$

where  $M$  denotes the number of nodes,  $w_i$  denotes the feature vector of the  $i$ -th node, and  $\parallel$  denotes concatenation.

6) Create hierarchical pooling architecture, as shown in Figure 1, and input the sum of the output of each readout layer to the linear layer for classification.

### 2.2.2 Sliding rules of multilayer supervised networks

In actual crisis supervision and prediction, we must use the dynamic sliding window method to train and test the network many times to ensure the validity of the SAGPOOL method. Specifically, the length of the training set was twice that of the test set and the slide window length. We set the length of the training set to 240-,120- and 60-day windows.

The main process of the dynamic sliding window method is illustrated in the Figure 2. Each paragraph (red vertical line) in Figure 2 represents a single network from the six-layer dynamic networks. For example, the networks in Figure 2 are the second-layer dynamic networks (PCC-PMFG). The tags (equal to 1) of each layer network correspond to the crisis event labels in Table 1 [49–51]. All other tags are equal to 0.

A general flow chart of MSNA method and the summary of this study are shown in Figure 3.

## 3 Data set

In this study, we chose 37 important stock markets<sup>1</sup> from four continents:Asia (15 stocks), Europe (12 stocks), America (9 stocks) and Oceania (1 stock). The detailed contents of the stocks is listed in Table 2.

Daily indices are considered, while the study period covers approximately 17 years from 1 January 2005, to 3 October 2021. The length of the closing price is 5,124.

<sup>1</sup> <https://www.wind.com.cn/NewSite/wft.html>.

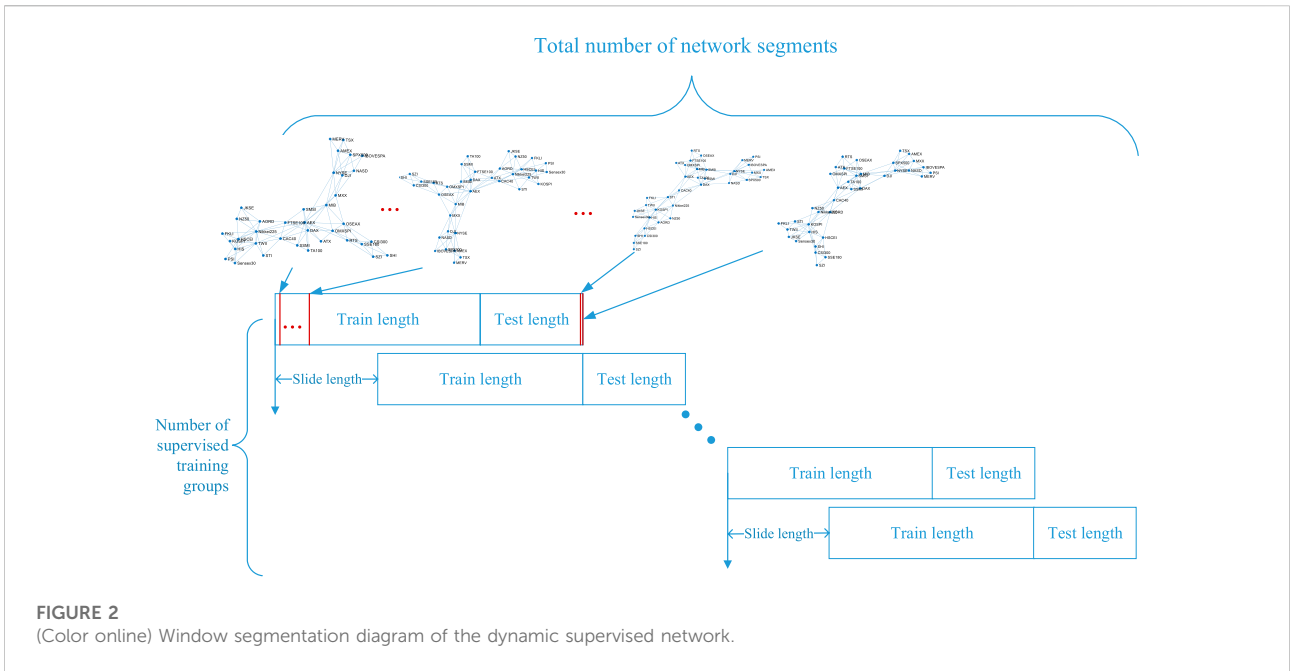


**FIGURE 2**  
(Color online) Window segmentation diagram of the dynamic supervised network.

**TABLE 1** The table of crisis events.

Crisis label	Crisis name	Start date	End date	Crisis event
C1	Subprime Mortgage	20/06/2007	10/03/2009	1
C2	European Sovereign Debt	20/04/2010	22/12/2011	1
C3	Russian Recession	18/03/2014	11/05/2015	1
C4	Stock Market Selloff	12/06/2015	27/06/2016	1
C5	Trade Conflict between China and the US	23/03/2018	11/10/2019	1
C6	US stock circuit breaker	20/01/2020	29/05/2020	1

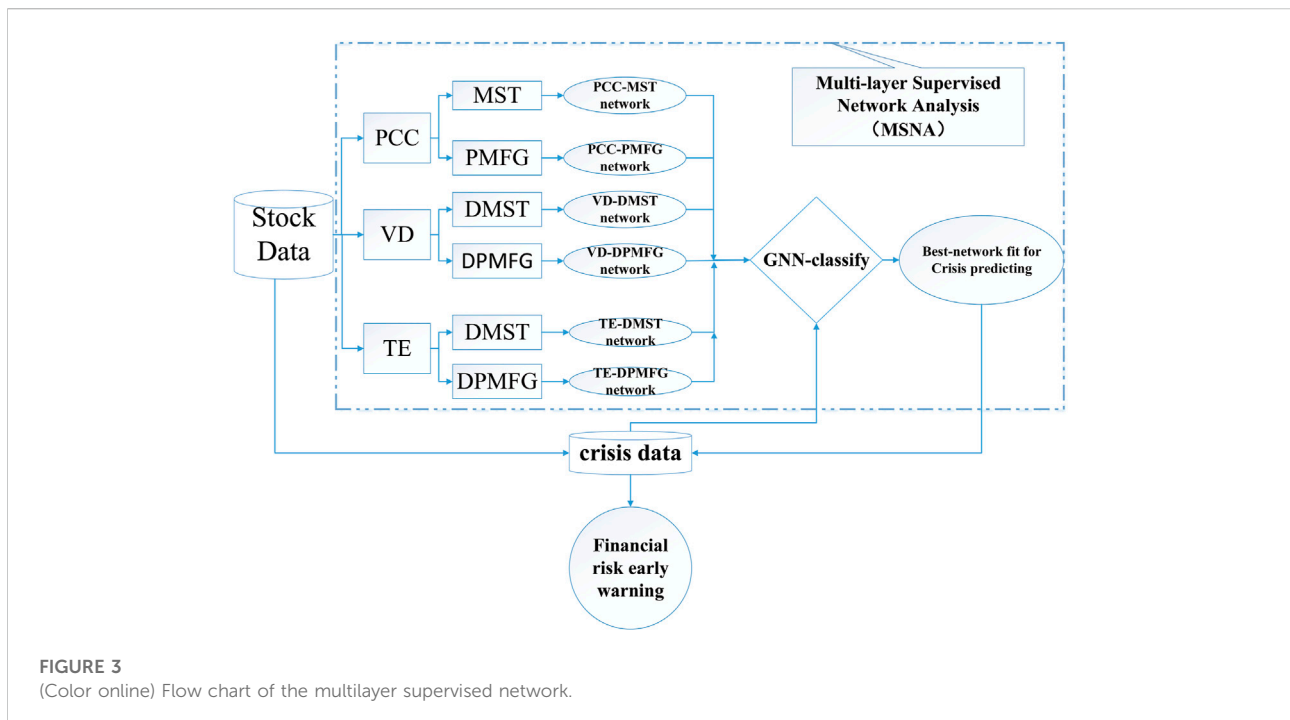


**FIGURE 3**  
(Color online) Flow chart of the multilayer supervised network.

TABLE 2 Stock index list.

Continent	Abbreviation of stock index	Country
Asia	KOSPI	Korea
	PSI	Philippine
	JKSE	Indonesia
	STI	Singapore
	Sensex30	India
	FKLI	Malaysia
	TA100	Israel
	Nikkei225	Japan
	TWII	Taiwan, China
	HIS	Hong Kong, China
	HSCEI	Hong Kong, China
	CSI 300	China mainland
	SZI	China mainland
	SSE180	China mainland
	SHI	China mainland
Europe	RTS	Russia
	NZ50	New Zealand
	SSMI	Switzerland
	OMXSPI	Sweden
	OSEAX	Norway
	AEX	Netherlands
	ATX	Austria
	MIB	Italy
	SMSI	Spain
	DAX	Germany
	CAC40	France
	FTSE100	United Kingdom
America	MERV	Argentina
	IBOVESPA	Brazil
	MXX	Mexico
	TSX	Canada
	AMEX	United States
	NYSE	United States
	NASD	United States
	SPX500	United States
DJI	United States	
Oceania	AORD	Australia

## 4 Result

### 4.1 Topology parameters and community structures of multilayer networks

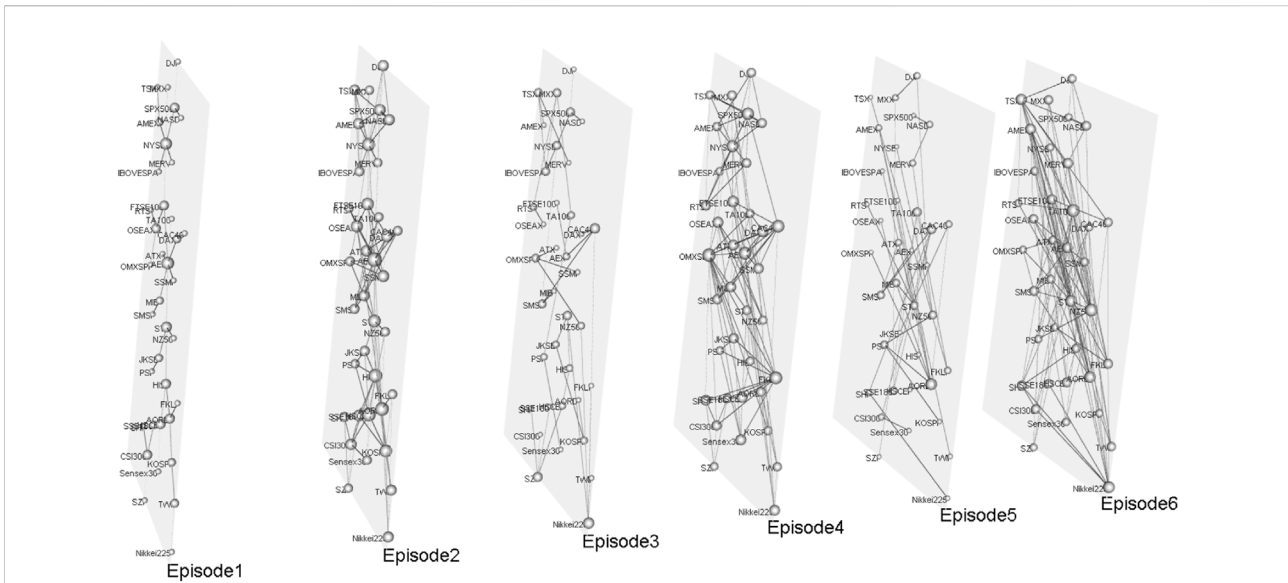
Based on multilayer network creation methods, we construct evolving 6-layer networks (PCC-MST,PCC-PMFG,VD-DMST,VD-DPMFG,TE-DMST,TE-DPMFG) on

240-, 120-, and 60-day windows. In this study, we set up  $\Delta = 1$ ,  $L = 120$ ,  $M = 37$ ,  $T = 5,123$ ,  $Q = 2$  and  $H = 4$ . The multiplex network of the global financial crisis shown in Figure 3. Figures 4, 5A,B show that DAX (Germany), SPX500 (United States) and STI (Singapore) have the larger degrees in the first layer network. Due to a broader amount of information in the second layer network, DAX (Germany), STI (Singapore), NYSE (United States) and HIS (Hong Kong, China) are all affected. In the third layer network, PSI (Philippine) is the head node of a directed spanning tree network owing to its comparatively earlier opening time, which is similar to Vrost et al [52, 53]. In the fourth-layer network, the NYSE and the SPX500 of the United States are the two most affected stock indices. As can be seen from the DMST in the fifth layer, the in-degree of HSCEI (Hong Kong, China) is zero, which indicates that the HSCEI is the least influenced stock. The most influenced node in the sixth layer network was NASD (United States).

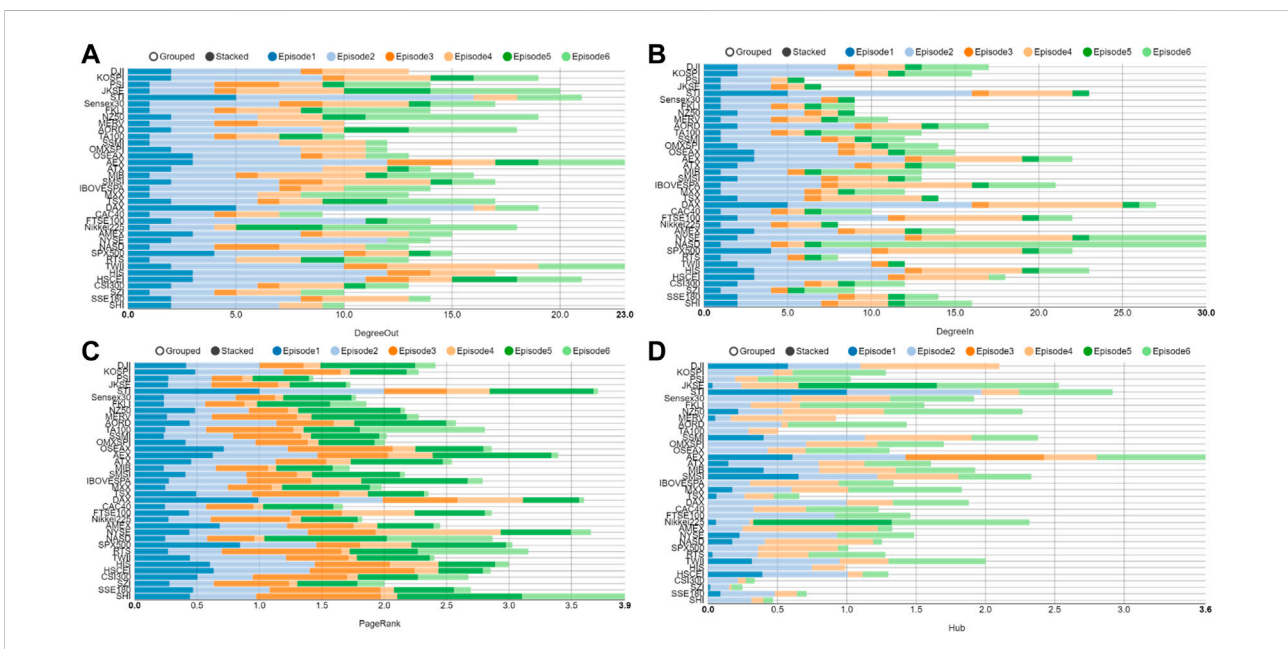
As can be seen from the cumulative PageRank values of each layer in Figure 5C, the PageRank values of SHI (China), STI (Singapore), DAX (Germany), and NASD (United States) are higher, which indicates that these stock indexes have strong dissemination power. In Figure 5D, AEX (United States) is at the hub node.

Although the parameters of the individual layer network can provide us with valuable information, the integration of multilayer network information is more important. The parameters of multilayer network at the time of the global financial crisis are shown in Figure 5. As shown in Figure 6A, the AEX (Netherlands), TWII (China), HSCEI (China), Tokyo (Japan) and STI (Singapore) are the most influential stocks. In Figure 6B, NYSE (United States), NASD (United States), STI (Singapore) and HIS (HongKong, China) are the most influenced stocks. From the PageRank index in Figure 6C, NYSE (United States), NASD (United States), SPX500 (United States) DAX (Germany) and SHI (China Mainland) are the most highly transmissible index. In Figure 6D, DAX (United States), AEX (United States), STI (Singapore), FTSE (Britain) are included as the main nodes in Hub index. Figure 6 shows that the results derived from the multilayer network ensemble parameters are more stable than those in the single layer network.

To analyze the community relationship of each node in the multilayer network, we use multilayer infomap algorithm [54] to detect the network's community structure. The results of the community division of the multilayer network are shown in Figure 7. Figure 6 shows the division of associations in each layer did not differ greatly, especially for layers 1–4. Asian stocks such as FKLI, KOSPI, TA100, Nikkei225, TWII, HIS, HSCEI, CSI300, SZI, SHI, Sensex30, STI belong to one community. The AORD (Australia) and NZ250 (New Zealand) belong to an other society. MXX, DJI, NYSE, NASD and SPX500 are all in one community



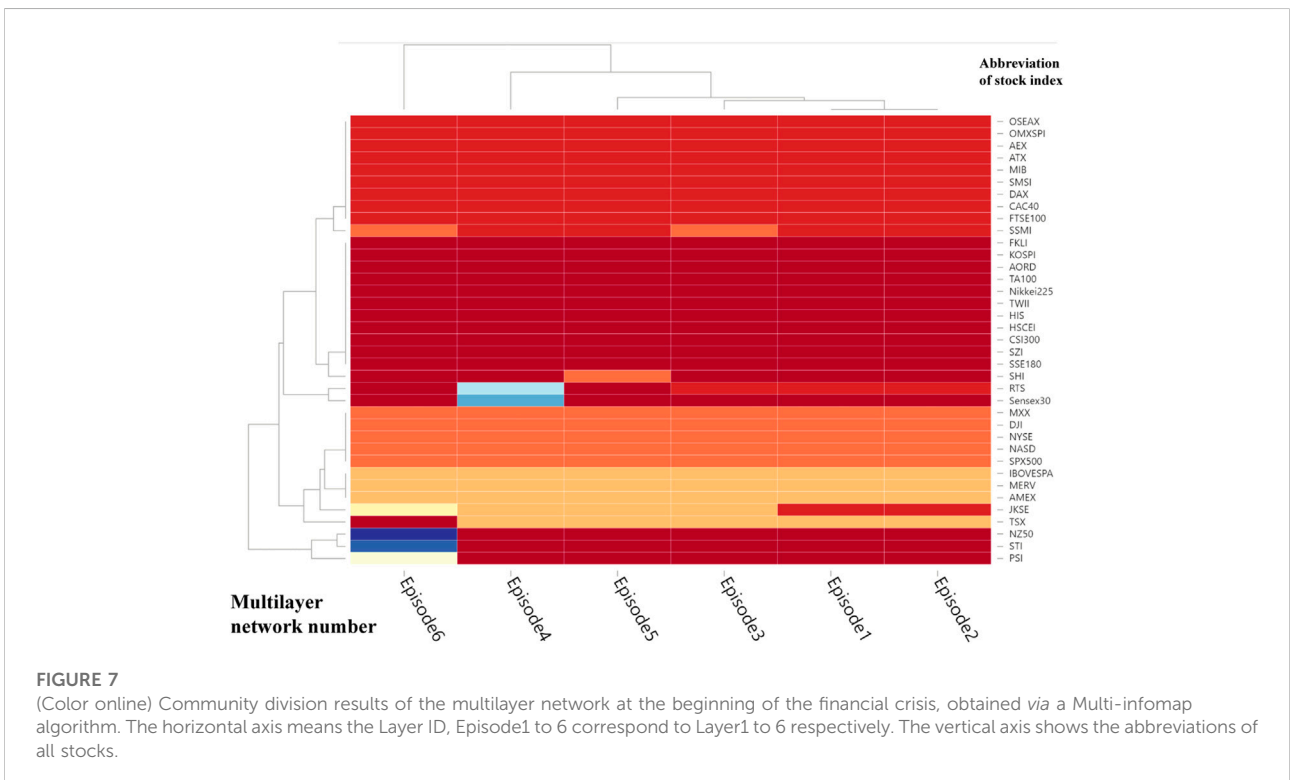
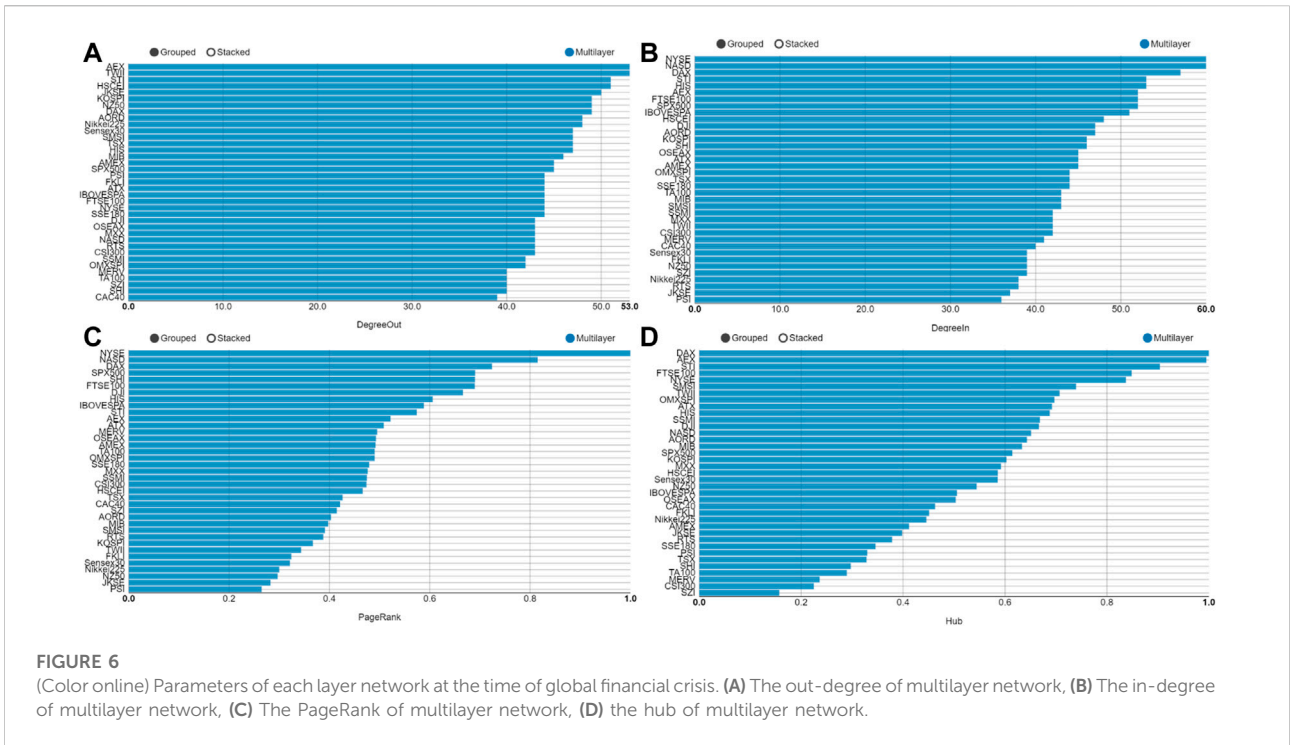
**FIGURE 4**  
(Color online) Multilayer network at the time of global financial crisis.



**FIGURE 5**  
(Color online) Parameters of each layer network at the time of global financial crisis. (A) The out-degree of each layer network; (B) The in-degree of each layer network; (C) The PageRank of each layer network; (D) The Hub of each layer network.

(American group-1). Ibovessa, Merv, AMEX and TSX belong to a single community (American group-2). OSEAX, OMXSPI, AEX, ATX, MIB, SMSI, DAX, CAC40, FTSE100, SSMI, and RTS are included in one community (the

European group). It also underscores that JKSE(Indonesia), of layers 1 and 2, belongs to the European group, while JKSE, of layers 3, 4 and 5 belongs to American group-2.



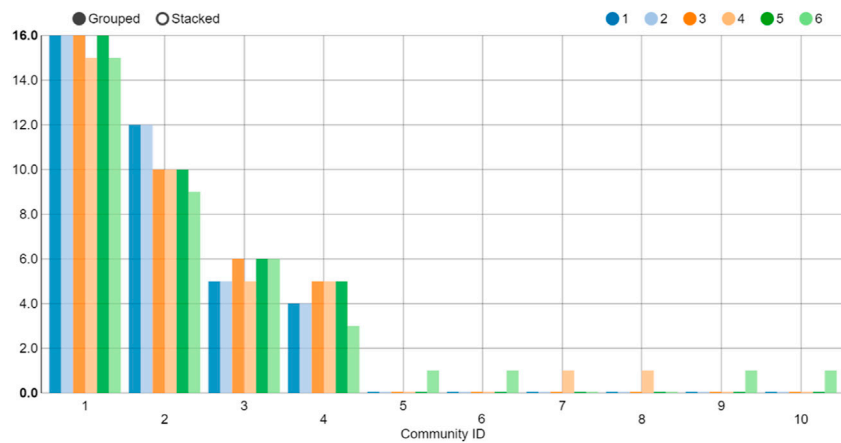


**FIGURE 8**  
(Color online) Quantity statistics in each community at the beginning of the global financial crisis. The horizontal axis indicates the community ID. The vertical axis represents quantities of each Community ID.

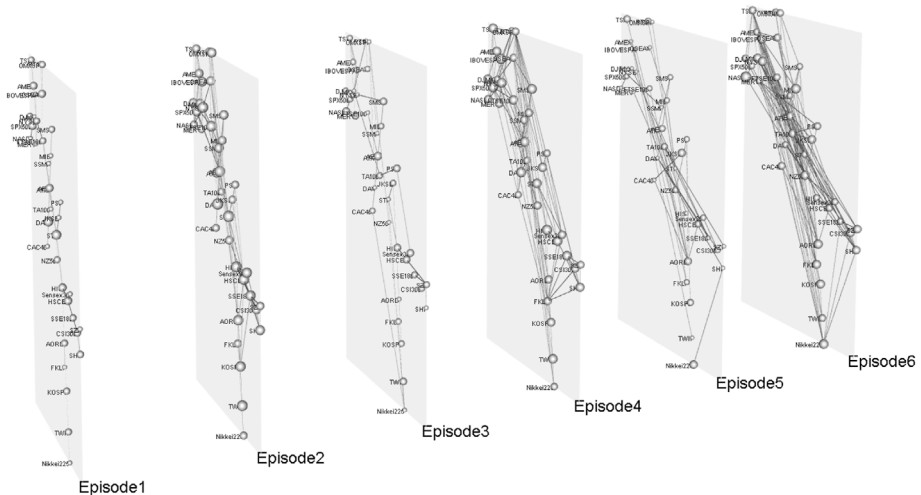


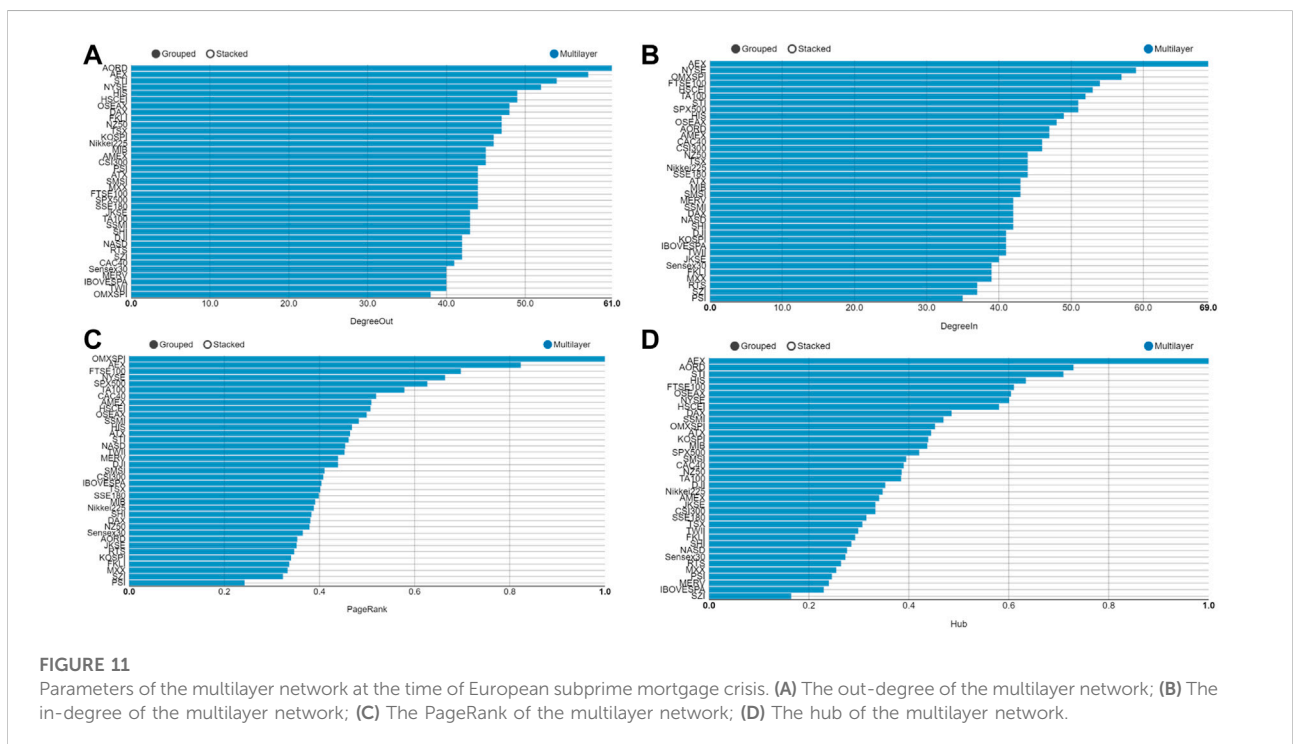
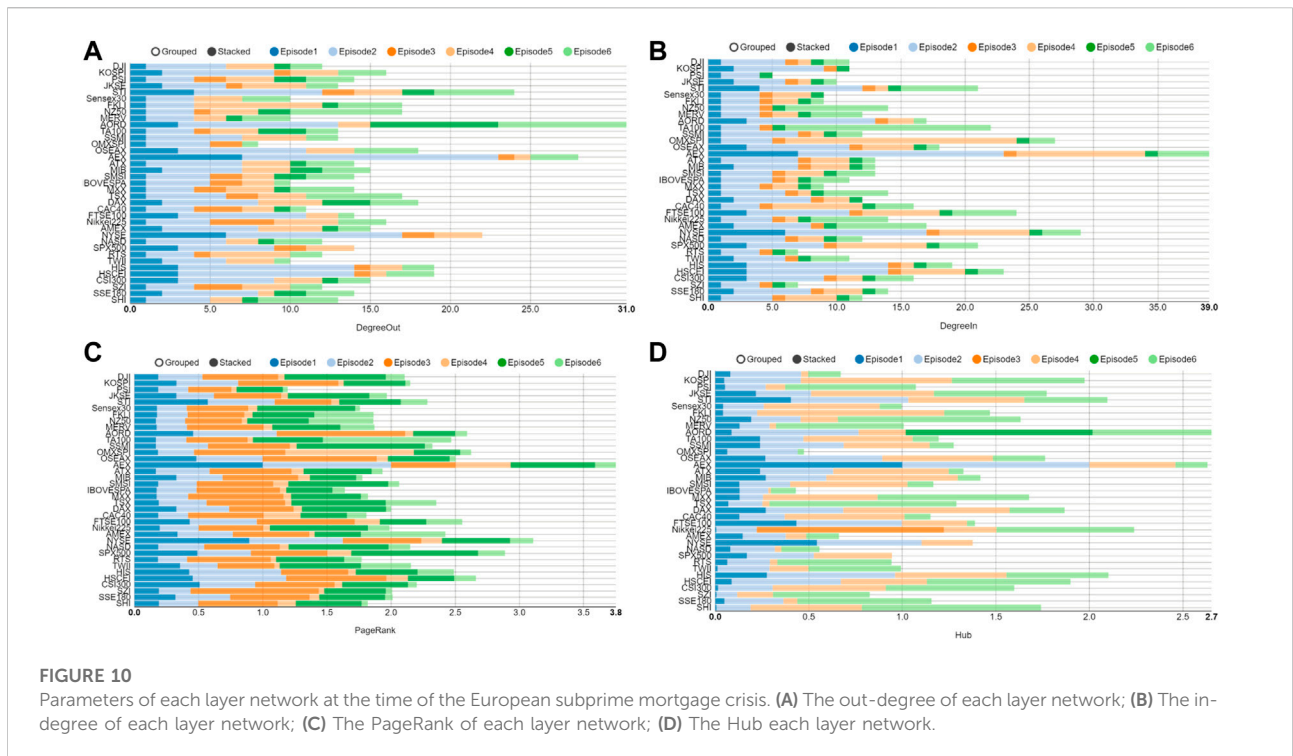
**FIGURE 9**  
(Color online) Multilayer network at the time of European subprime mortgage crisis.

In Figure 7, the findings from the distribution of communities indicate that the layer 1(PCC-MST) and layer 2(PCC-PMFG) belong to one community. In addition, the layer 3(VD-DMST) and layer 5 (TE-DMST) are similar to layers 1 and 2. The stock numbers for each community are shown in Figure 8. Communities 1 to 4 correspond to the Asian-Oceania group, European group, American group 1 and American group 2, respectively.

We also show the multiplex network and its parameters of the European subprime mortgage crisis in Figures 9, 10, respectively. As shown in Figures 8, 10A, AEX and NYSE

are most influenced in the first layer network. AEX, NYSE, HIS and HSCEI of the second-layer network are most influenced. Because of the early opening, PSI is the most influential stock in the third-layer network. OMXSPI (Sweden) is the most influenced stock in the fourth-layer network. In the fifth-layer network, AORD (Australia) is the most influential stock. In the sixth layer network, the most influenced stock was TA100 (Israel).

In Figure 10C, AEX (Netherlands),NYSE (United States), SPX500 (United States) and HSCEI (China) have a strong infectivity. The hub nodes in Figure 10D are AORD



(Australia), AEX (Netherlands), Nikkei225 (Japan) and HIS (China). It can be surmised, by uniting the results of Figures 9, 10 that the European stocks (AEX,OMXSPI) are the most affected

and infected during the European subprime mortgage crisis. Due to early opening time of AORD (Australia), PSI (Philippines), and Nikkei225, they have the most influential effect.

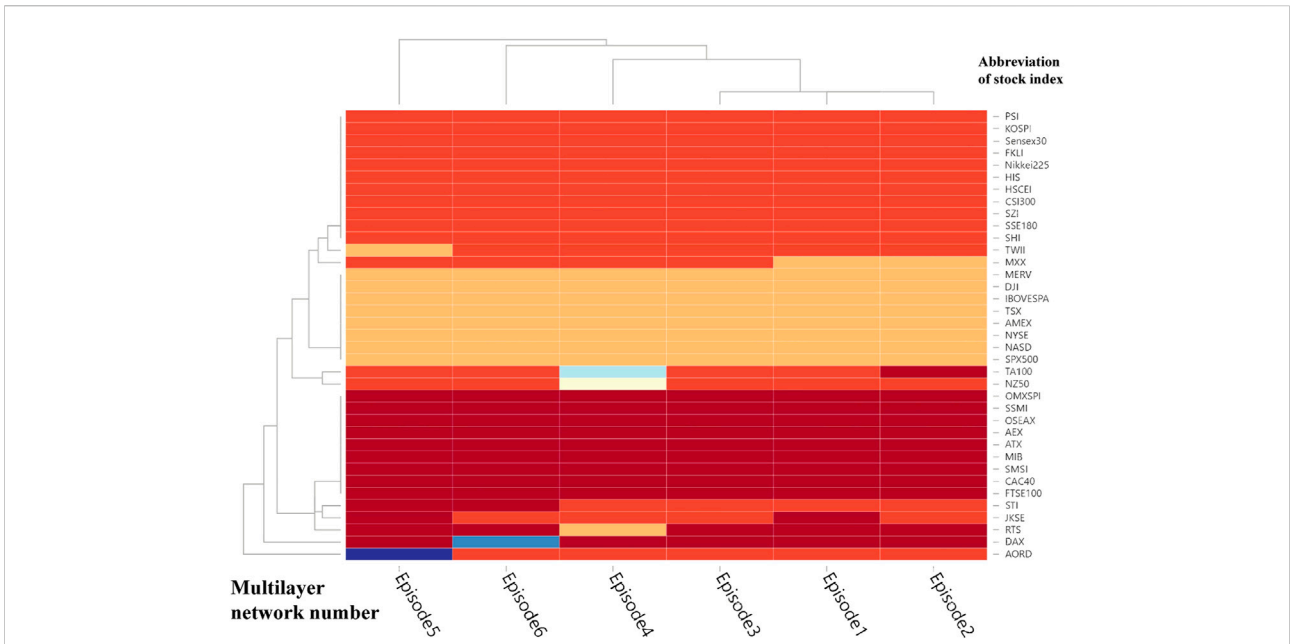


**FIGURE 12**  
Community division results of the multilayer network at the beginning of the European subprime mortgage crisis, obtained by a multi-infomap algorithm.

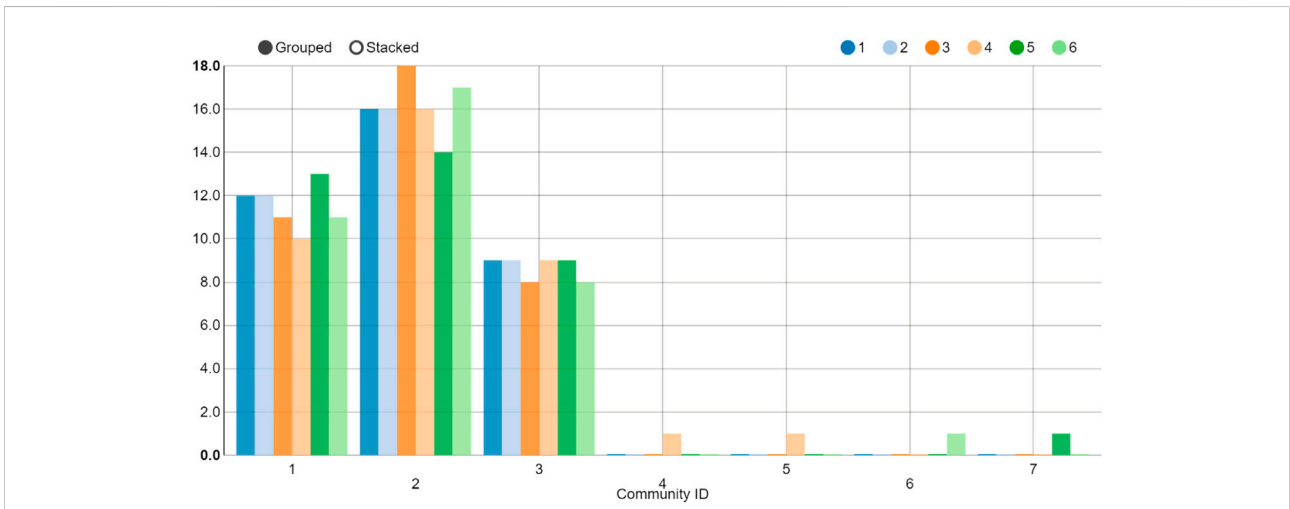


**FIGURE 13**  
Quantity statistics in each community at the beginning of the European subprime mortgage crisis. The horizontal axis means the Community ID. The vertical axis indicates quantities of each Community ID.

The multilayer result during the European subprime mortgage crisis is depicted in Figure 11. The out-/in-degree, PageRank and Hub of AEX (Netherlands) and OMXSPI (Sweden) are all at the forefront. We also present the community division results of the multilayer in Figures 12, 13. The biggest difference between Figures 7, 12 is that MXX, DJI, NYSE, NASD, SPX500, Ibovessa, Merv, AMEX and TSX

belong to one community (the American group) during the European subprime mortgage crisis but belong to two communities (American society-1 and 2) in the Global financial crisis. Further conclusions are illustrated in Figures 8, 13 show that the number of communities in the period of global financial crisis is higher than that in the period of European subprime mortgage crisis period.

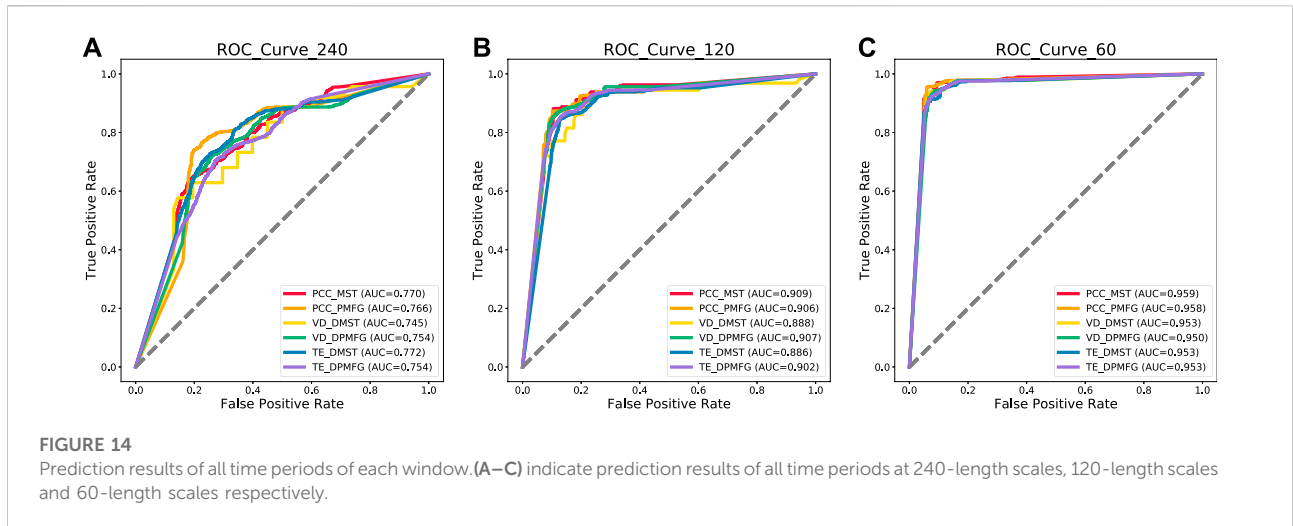


TABLE 3 Mean results of each multilayer networks using MSNA methods.

	mean_total_240			mean_total_120			mean_total_60		
	Accuracy	Recall	f1_score	Accuracy	Recall	f1_score	Accuracy	Recall	f1_score
Mul1	0.7105	0.6886	0.7027	0.8800	0.8637	0.8732	0.9344	0.9338	0.9308
Mul2	0.7682	0.7492	0.7625	0.8798	0.8589	0.8724	0.9358	0.9239	0.9315
Mul3	0.6665	0.6804	0.6696	0.8204	0.8155	0.8129	0.9319	0.9320	0.9282
Mul4	0.7227	0.7342	0.7245	0.8737	0.8624	0.8672	0.9262	0.9183	0.9216
Mul5	0.7357	0.7191	0.7300	0.8580	0.8422	0.8502	0.9193	0.9118	0.9144
Mul6	0.7128	0.7303	0.7165	0.8605	0.8465	0.8531	0.9217	0.9282	0.9181

TABLE 4 The mean results of each multilayer network of the six crises in the 240-day window.

L240	Mul1	Mul2	Mul3	Mul4	Mul5	Mul6	MeanC
c1	0.5736	0.6611	0.6653	0.6944	0.6917	0.6819	0.6613
c2	0.6000	0.6983	0.5333	0.6850	0.6567	0.6700	0.6406
c3	0.5708	0.5875	0.5417	0.6021	0.5917	0.5899	0.5806
c4	0.7750	0.7750	0.7750	0.7750	0.7472	0.7389	0.7644
c5	0.6850	0.7083	0.6216	0.6483	0.6150	0.6583	0.6561
c6	0.7583	0.7500	0.7333	0.6000	0.8250	0.7083	0.7292
Mean Mul	0.6605	0.6967	0.6450	0.6675	0.6879	0.6745	

### 4.2 Crisis early warning results based on multilayer supervision networks

Based on the created dynamic multilayer network, we intend to add the crisis events as label values and integrate the supervised characteristics to each dynamic network layer. Because of the weakness of machine learning and neural

network in handling feature representation of input dynamic networks, we utilize the GNNC method to fill this technical gap. Specifically, we train and test all six-layer dynamic networks utilizing our MSNA method in 60-day, 120-day and 240-day windows. The detailed results of the three windows are shown in Figure 14 and Table 3. The mean-total-240, mean-total-120, mean-total-60 in Table 3 indicate

TABLE 5 The mean results of each multilayer network of the six crises in the 120-day window.

L120	e1	e2	e3	e4	e5	e6	meanC
c1	0.8050	0.8967	0.7983	0.8183	0.8333	0.8333	0.8308
c2	0.9148	0.8130	0.8130	0.9019	0.8296	0.8852	0.8596
c3	0.6833	0.7714	0.7976	0.8095	0.8286	0.7095	0.7667
c4	0.9222	0.9000	0.9000	0.8944	0.8556	0.8667	0.8898
c5	0.8019	0.7352	0.6907	0.7481	0.7648	0.7500	0.7485
c6	0.7750	0.6750	0.4667	0.6333	0.6000	0.7083	0.6431
mean E	0.8170	0.7985	0.7444	0.8010	0.7853	0.7921	

TABLE 6 The mean results of each multilayer network of the six crises in the 60-day window.

L60	e1	e2	e3	e4	e5	e6	meanC
c1	0.8983	0.8700	0.8967	0.8983	0.8983	0.8900	0.8919
c2	0.8789	0.8807	0.9140	0.9053	0.8772	0.8825	0.8898
c3	0.9359	0.9256	0.9179	0.8846	0.8487	0.8872	0.9000
c4	0.8389	0.8861	0.8444	0.8806	0.8611	0.9167	0.8713
c5	0.9078	0.8863	0.8745	0.8843	0.8843	0.8961	0.8889
c6	0.8333	0.7444	0.7333	0.4667	0.7333	0.7000	0.7019
mean E	0.8822	0.8655	0.8635	0.8200	0.8505	0.8621	

the mean precision results of MSNA method in 240-,120- and 60-day windows, respectively.

As shown in Table 3 and Figure 14, the accuracy of financial crisis prediction increases with the reduction of window length. In general, accuracy can properly evaluate the model performance. It represents the prediction correctness of crisis events and non crisis events (all events). Recall indicates the prediction precision of all crisis events. When the model deals with unbalanced sample classification, f1\_score can more correctly evaluate the model performance than accuracy and recall. For an ideal early warning model, accuracy, recall and f1\_score should be as large as possible. As can be seen from Table 3, when the time window is 60, the lowest f1\_score (Mul5) also reaches 0.9144. While the window is 240, the lowest layer (Mul3) is 0.6665. This result confirms the effectiveness of our MSNA method in short sequence crisis prediction. In addition, we also discovered that the fifth-layer (TE-DMST) network has the best performance in a long windows, while the first-layer (PCC-MST) network has the best results in short windows.

Simultaneously, we also intercepted warning results of six periods of financial crisis for statistics. The detailed results of accuracy and ROC curve are displayed in Tables 4–6 and Figures 15–17. Table 6 shows that, in the 240-day window condition, the best performances of the six financial crises prediction are Mul4 (VD-PMFG), Mul2 (PCC-PMFG), Mul4,

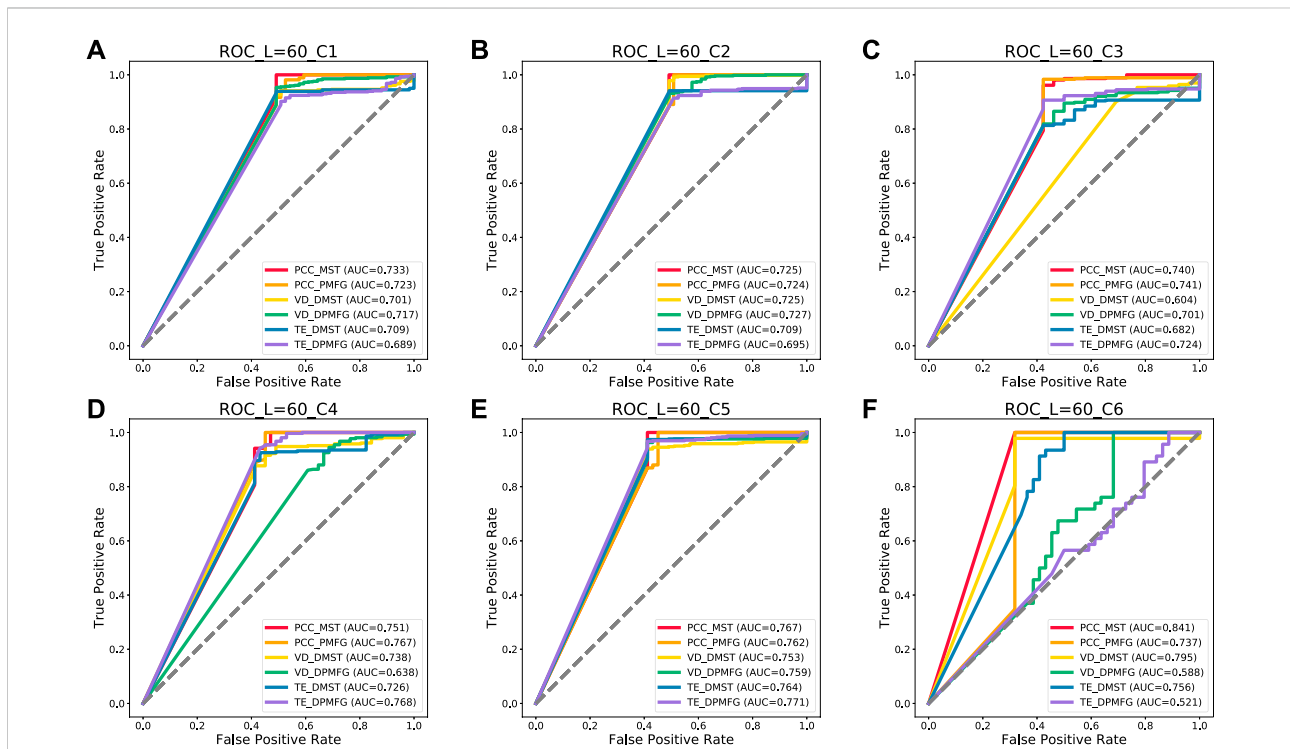
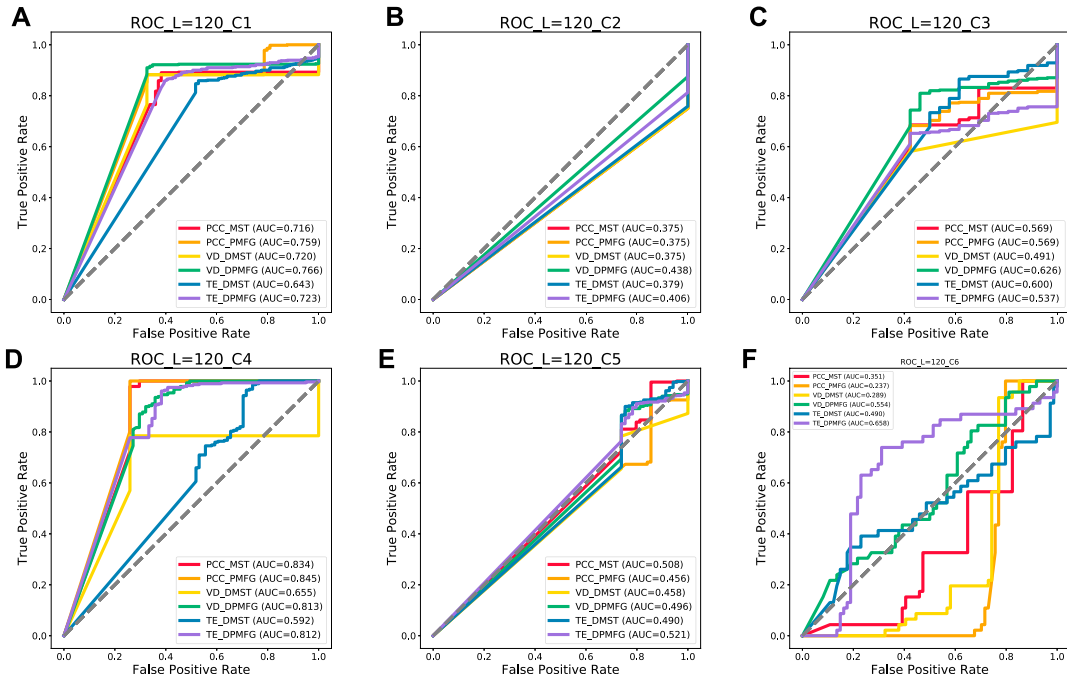
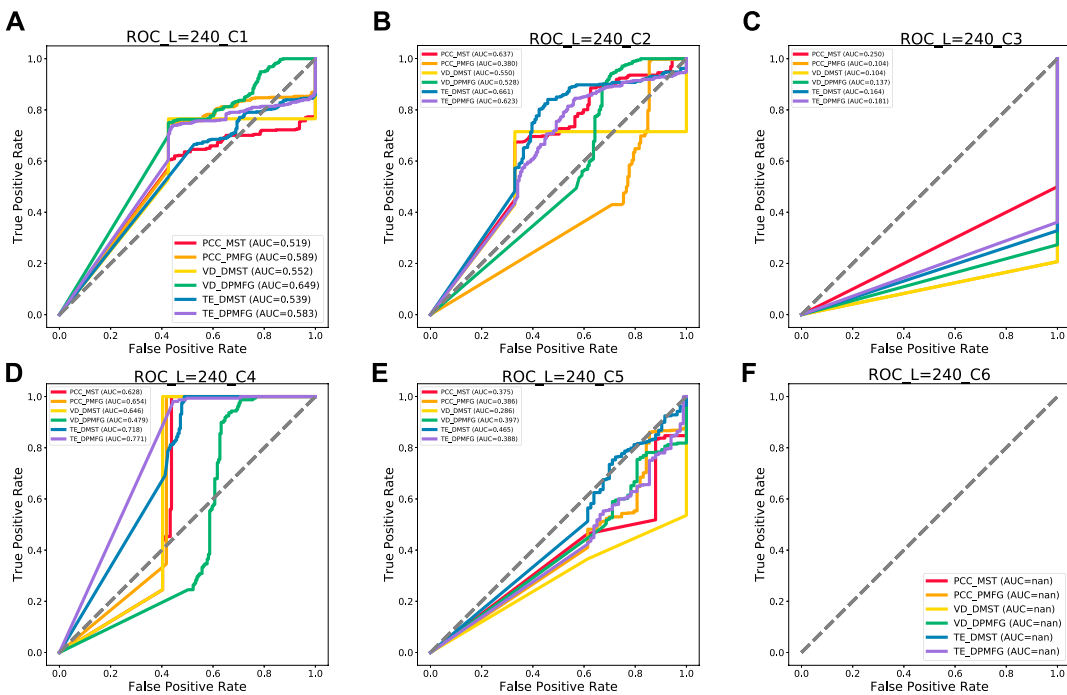


FIGURE 15 Prediction of the six crises of each layer network at 60-day windows. (A–F) indicate the prediction result of each financial crisis. C1 to C6 indicate the following crises: Subprime Mortgage, European Sovereign Debt, Russian Recession, Stock Market Selloff, and Trade Conflict between China and the United States, US stock circuit breaker, respectively.



**FIGURE 16**

Prediction results of each layer of the network at 120-day windows. (A–F) indicate the prediction result of each financial crisis. C1 to C6 indicate the following crises: Subprime Mortgage, European Sovereign Debt, Russian Recession, Stock Market Selloff, and Trade Conflict between China and the United States, US stock circuit breaker, respectively.



**FIGURE 17**

Prediction results of each layer of the network at 240-day windows. (A–F) indicate prediction result of each financial crisis. C1–C6 indicate the following crises: Subprime Mortgage Crisis, European Sovereign Debt, Russian Recession, Stock Market Selloff, and Trade Conflict between China and the United States, US stock circuit breaker, respectively.

Mul4, Mul2, and Mul4, respectively. In Table 5 corresponding to 120-length condition, we discover that Mul2 (PCC-DPMFG), Mul1 (PCC-DMST), Mul5 (TE-DMST), Mul1, Mul1, Mul1 have the best performances of 6 financial crises (c1 to c6) prediction, respectively. Table 6 is the result of the accuracy of six financial crisis predictions in a 60-length condition. We can conclude that Mul1, Mul4, Mul1, Mul6, Mul1, and Mul1 have the best performances of the 6 financial crisis (c1 to c6) predictions, respectively. The optimal mean values of the accuracy of the six crises from 240-length to 60-day are Mul2, Mul1, and Mul1, respectively. In summary, the correlation network is the most accurate system for predicting financial crises.

As can be seen in Figure 15, the PCC-MST, VD-DPMFG, PCC-PMFG, PCC-MST, TE-DPMFG, and PCC-MST networks are the most stable and efficient graphs for predicting the six financial crises of 60-day condition, respectively. In Figures 16, 17, the results of the AUC values in the 120- and the 240-day conditions were not all stable and efficient. In the 120-day condition, there are five efficient networks (VD-DPMFG, VD-DPMFG, PCC-PMFG, PCC-MST, TE-DPMFG) corresponding to c1, c3, c4, c5, and c6, respectively. In the 240-length condition, there are only three efficient networks (VD-DPMFG, PCC-MST, TE-DPMFG) corresponding to c1, c2, and c4, respectively.

## 5 Conclusion and discussion

Several scholars have proposed various effective methods for financial network construction. For example, Gan et al. applied the threshold method to reduce noise in a Pearson correlation network [55]. Further, Marti et al. proposed using the MST method and PCC to construct the network, which resolved the shortcomings of artificial and subjective threshold selection, and likewise simplified the topology of the financial network (M-1) [56]. Because the MST method will result in a loss of important information, Hosseini et al. proposed constructing it using PCC and PMFG (3M-6) [57]. Because there are many nonlinear relationships between financial institutions, analyzing only linear relationships will result in a loss of important information. Therefore, Hosseini et al. applied the TE method to investigate the relationship between several stocks, and utilized DMST to construct the network [58]. Zhang et al. constructed a financial network by employing VD method [59]. Additionally, some scholars have used DCC GARCH t copula [60], GARCH BEKK model [61], symbolic dynamics model [62], and nonlinear Granger causality tests [63] to build financial networks.

In this study, we employed PCC, VD, TE, MST, PMFG, DMST, and DPMFG, which are popular among the above methods, to construct a six-layer dynamic financial network. Through the analysis of topological quantities (degree, out/in-degree, PageRank, Hub, etc.) in multilayer networks, we conclude

that in the stage of global financial crisis, the external risk contagion effect and affected intensity of the United States, China, Japan and Singapore were comparatively large. At the stage of the European subprime mortgage crisis, Australia, the Netherlands and Singapore had the greatest external impact, while the Netherlands, the United States, Sweden and the United Kingdom were the most affected. The community division results of the multilayer network show that the community number during the global financial crisis (four communities) was lower than that during the European subprime mortgage crisis (three communities). In short, we use the topological features of the information spillover network between stock indices in various essential places as a training element to improve existing macroeconomic-based warning indicators. The proposed MSNA early warning model, with a multi-layer information spillover network as input variable, has shown excellent early warning effect in empirical studies on real-world datasets and can provide strategic support to regulatory authorities to prevent financial crises.

Further research should be conducted to enhance the accuracy of long-term crisis warning, which is affected by the amount of training data, model overfitting and other factors. For the problem of training set data volume, we will unite the macroeconomic data, sentiment indices and other data in the future, and merge the mixed frequency model [64] to reduce the impact of the data volume of the training set. For model overfitting, we will improve model's prediction accuracy in the future by adjusting its regularization.

## Data availability statement

Publicly available datasets were analyzed in this study. This data can be found here: <https://www.wind.com.cn/NewSite/wft.html>.

## Author contributions

LQ determined the research problems and objectives. LQ and RS analyzed the data and wrote the manuscript. ZW supervised the study and designed project. The authors contributed to manuscript revision and have read approved the submitted version.

## Funding

This research was funded by the General project of NSFC: Research on multi-dimensional and multiple contagions of Banking Systemic Financial Risk in structural change (Grant Number. 71973098) and Youth project of NSFC: Financial risk

early-warning based on high dimensional supervised network (Grant Number. 12105178).

## Conflict of interest

The authors declare that the research was conducted in the absence of any commercial or financial relationships that could be construed as a potential conflict of interest.

## References

- Frankel JA, Rose AK. Currency crashes in emerging markets: An empirical treatment. *J Int Econ* (1996) 41(3):351–66. doi:10.1016/S0022-1996(96)01441-9
- Kaminsky G, Lizondo S, Reinhart CM. Leading indicators of currency crises. *Staff Pap Int Monet Fund* (1998) 45(1):1–48. doi:10.2307/3867328
- Berg A, Pattillo C. Predicting currency crises. *J Int Money Finance* (1999) 18(4):561–86. doi:10.1016/S0261-5606(99)00024-8
- Sachs JD, Tornell A, Velasco A, Calvo GA, Cooper RN. Financial crises in emerging markets: The lessons from 1995. *Brookings Pap Econ Act* (1996) 1996(1):147–215. doi:10.2307/2534648
- Billio M, Casarin R, Costola M, Pasqualini A. An entropy-based early warning indicator for systemic risk. *J Int Financial Markets Institutions Money* (2016) 45:42–59. doi:10.1016/j.intfin.2016.05.008
- Dastkhan H. Network-based early warning system to predict financial crisis. *Int J Fin Econ* (2019) 26(1):594–616. doi:10.1002/ijfe.1806
- Kumar M, Moorthy U, Perraudin W. Predicting emerging market currency crashes. *J Empir Finance* (2003) 10(4):427–54. doi:10.1016/S0927-5398(02)00068-3
- Klomp J. Causes of banking crises revisited. *North Am J Econ Finance* (2009) 21(1):72–87. doi:10.1016/j.najef.2009.11.005
- Schularick M, Taylor AM. Credit booms gone bust: Monetary policy, leverage cycles, and financial crises, 1870–2008. *Am Econ Rev* (2012) 102(2):1029–61. doi:10.1257/aer.102.2.1029
- Greenwood R, Hanson SG, Sheifer A, Sorensen JA. Predictable financial crises [J]. *J Financ* (2022) 77(2):863–921. doi:10.1111/jofi.13105
- Boonman TM, Jacobs J, Kuper GH, Romero A. Early warning systems for currency crises with real-time data. *Open Econ Rev* (2019) 30(4):813–35. doi:10.1007/s11079-019-09530-0
- Sornette D, Demos G, Zhang Q, Cauwels P, Zhang Q. Real-time prediction and post-mortem analysis of the Shanghai 2015 stock market bubble and crash. *J Invest Strateg* (2015) 4:77–95. doi:10.21314/jois.2015.063
- Fricke D. Financial crisis prediction: A model comparison. *SSRN J* (2017) 3059052:1–9. doi:10.2139/ssrn.3059052
- Tölö E. Predicting systemic financial crises with recurrent neural networks. *J Financial Stab* (2020) 49:100746–19. doi:10.1016/j.jfs.2020.100746
- Zhu ZY, Liu N. Early warning of financial risk based on K-means clustering algorithm. *Complexity* (2021) 24:1–12. doi:10.1155/2021/5571683
- Liu LB, Chen C, Wang B. Predicting financial crises with machine learning methods. *J Forecast* (2022) 41(5):871–910. doi:10.1002/for.2840
- Bouchaud JP. Economics needs a scientific revolution. *Nature* (2008) 455(7217):1181. doi:10.1038/4551181a
- Farmer JD, Foley D. The economy needs agent-based modelling. *Nature* (2009) 460(7256):685–6. doi:10.1038/460685a
- Catanzaro M, Buchanan M. Network opportunity. *Nat Phys* (2013) 9(3):121–3. doi:10.1038/nphys2570
- Battiston S, Farmer JD, Flache A, Garlaschelli D, Haldane AG, Heesterbeek H, et al. Complexity theory and financial regulation: Economic policy needs interdisciplinary network analysis and behavioral modeling[J]. *Science* (2016) 351(6275):818–9. doi:10.1126/science.aad0299
- Kumar S, Deo N. Correlation and network analysis of global financial indices. *Phys Rev E* (2012) 86:026101–8. doi:10.1103/PhysRevE.86.026101
- Dima B, Dima SM. Mutual information and persistence in the stochastic volatility of market returns: An emergent market example. *Int Rev Econ Finance* (2017) 51:36–59. doi:10.1016/j.iref.2017.05.008
- Brunetti C, Harris JH, Mankad S, Michailidis G. Interconnectedness in the interbank market. *J Financ Econ* (2019) 133(2):520–38. doi:10.1016/j.jfineco.2019.02.006
- Zhang X, Podobnik B, Kenett DY, Stanley HE. Systemic risk and causality dynamics of the world international shipping market. *Physica A: Stat Mech its Appl* (2014) 415:43–53. doi:10.1016/j.physa.2014.07.068
- Qiu L, Yang H. Transfer entropy calculation for short time sequences with application to stock markets. *Physica A: Stat Mech its Appl* (2020) 559:125121–0. doi:10.1016/j.physa.2020.125121
- Diebold FX, Yilmaz K. On the network topology of variance decompositions: Measuring the connectedness of financial firms. *J Econom* (2014) 182(1):119–34. doi:10.1016/j.jeconom.2014.04.012
- Yang Y, Yang H. Complex network-based time series analysis. *Physica A: Stat Mech its Appl* (2007) 387(5):1381–6. doi:10.1016/j.physa.2007.10.055
- Yang C, Zhu X, Li Q, Chen Y, Deng Q. Research on the evolution of stock correlation based on maximal spanning trees. *Physica A: Stat Mech its Appl* (2014) 415:1–18. doi:10.1016/j.physa.2014.07.069
- Wang GJ, Xie C, Stanley HE. Correlation structure and evolution of world stock markets: Evidence from Pearson and partial correlation-based networks. *Comput Econ* (2018) 51(3):607–35. doi:10.1007/s10614-016-9627-7
- Tumminello M, Aste T, Matteo TD, Mantegna RN. A tool for filtering information in complex systems. *Proc Natl Acad Sci U S A* (2005) 102(30):10421–6. doi:10.1073/pnas.0500298102
- Kwon O, Yang JS. Information flow between stock indices. *Europhys Lett* (2008) 82(6):68003. doi:10.1209/0295-5075/82/68003
- Fiedor P. Networks in financial markets based on the mutual information rate. *Phys Rev E* (2014) 89(5):052801–7. doi:10.1103/PhysRevE.89.052801
- Park D, Ryu D. Forecasting stock market dynamics using bidirectional long short-term memory. *Rom J Econ Forecast* (2021) 24:22–34.
- McBeth MK, Tokle RJ, Schaefer S. Media narratives versus evidence in economic policy making: The 2008–2009 financial crisis\*. *Soc Sci Q* (2018) 99(2):791–806. doi:10.1111/ssqu.12456
- Samitas A, Kampouris E, Kenourgios D. Machine learning as an early warning system to predict financial crisis. *Int Rev Financ Anal* (2020) 71:101507. doi:10.1016/j.irfa.2020.101507
- Zhang X, Chen MY, Wang MG, Ge YE, Stanley HE. A novel hybrid approach to Baltic Dry Index forecasting based on a combined dynamic fluctuation network and artificial intelligence method. *APPL MATH COMPUT* (2019) 361:499–516. doi:10.1016/j.amc.2019.05.043
- Lee J, Lee I, Kang J. Self-attention graph pooling. In: 36th International Conference on Machine Learning; Long Beach, CA (2019). ICML 6661–6670.
- Ying R, Morris C, Hamilton WL, You J, Ren X, Leskovec J. Hierarchical graph representation learning with differentiable pooling. *Adv Neural Inf Process Syst* (2018) 38:4800–10. doi:10.48550/arXiv.1806.08804
- Qiu L, Nan WY. Brain network constancy and participant recognition: An integrated approach to big data and complex network analysis. *Front Psychol* (2020) 11:1003–24. doi:10.3389/fpsyg.2020.01003
- Gabow HN, Galil Z, Spencer T, Tarjan RE. Efficient algorithms for finding minimum spanning trees in undirected and directed graphs. *Combinatorica* (1986) 6:109–22. doi:10.1007/BF02579168
- Sandoval L. Structure of a global network of financial companies based on transfer entropy. *Entropy* (2014) 16(8):4443–82. doi:10.3390/e16084443

## Publisher's note

All claims expressed in this article are solely those of the authors and do not necessarily represent those of their affiliated organizations, or those of the publisher, the editors and the reviewers. Any product that may be evaluated in this article, or claim that may be made by its manufacturer, is not guaranteed or endorsed by the publisher.

42. De Domenico M, Solé-Ribalta A, Cozzo E, Kivela M, Moreno Y, Porter MA, et al. Mathematical formulation of multilayer networks. *Phys Rev X* (2013) 3(4):041022–15. doi:10.1103/PhysRevX.3.041022
43. Bargigli L, di Iasio G, Infante L, Lillo F, Pierobon F. The multiplex structure of interbank networks. *Quant Finance* (2015) 15(4):673–91. doi:10.1080/14697688.2014.968356
44. De Domenico M, Solé-Ribalta A, Omodei E, Gómez S, Arenas A. Ranking in interconnected multilayer networks reveals versatile nodes. *Nat Commun* (2015) 6:6868–6. doi:10.1038/ncomms7868
45. Boccaletti S, Bianconi G, Criado R, Del Genio CI, Gómez-Gardeñes J, Romance M, et al. The structure and dynamics of multilayer networks. *Phys Rep* (2014) 544(1):121–2. doi:10.1016/j.physrep.2014.07.001
46. Cao Y, Liu Z, Li C, Liu Z, Li J, Chua TS. Multi-channel graph neural network for entity alignment[J]. In: ACL 2019-57th Annual Meeting of the Association for Computational Linguistics, Proceedings of the Conference; 2019 Jul 28–Aug 2; Florence, Italy (2020). p. 1452–61. doi:10.18653/v1/p19-1140
47. Kipf TN, Welling M. Semi-supervised classification with graph convolutional networks[J]. In 5th International Conference on Learning Representations ICLR 2017 - Conference Track Proceedings; 2017 Apr 24–26; Toulon, France (2017).
48. Xu K, Li C, Tian Y, Sonobe T, Kawarabayashi KI, Jegelka S. Representation learning on graphs with jumping knowledge networks[J]. In: 35th International Conference on Machine Learning; 2018 Jul 10–15; Stockholm, Sweden (2018). p. 8676–85.
49. Tommaso B. Systemic risk. GitHub (2022). Available from: <https://github.com/TommasoBelluzzo/SystemicRisk/releases/tag/v3.5.0> (Accessed May 18, 2022).
50. Zhu M, Xu ZX. The impact of the China US trade tensions on China's stock market. *Stud Int Finance* (2021) 43–12. doi:10.16475/j.cnki.1006-1029.2021.04.001-en
51. Cortes F, Lindner P, Malik S, Segoviano Basurto M. A comprehensive multi-sector tool for analysis of systemic risk and interconnectedness (SyRIN). *IMF Work Pap* (2018) 18(14):1–54. doi:10.5089/9781484338605.001
52. Baumöhl E, Kočenda E, Lyócsa Š, Výrost T. Networks of volatility spillovers among stock markets. *Physica A: Stat Mech its Appl* (2018) 490(C):1555–74. doi:10.1016/j.physa.2017.08.123
53. Výrost T, Lyócsa Š, Baumöhl E. Granger causality stock market networks: Temporal proximity and preferential attachment. *Physica A: Stat Mech its Appl* (2015) 427:262–76. doi:10.1016/j.physa.2015.02.017
54. De Domenico M, Lancichinetti A, Arenas A, Rosvall M. Identifying modular flows on multilayer networks reveals highly overlapping organization in interconnected systems. *Phys Rev X* (2015) 5(1):011027–11. doi:10.1103/PhysRevX.5.011027
55. Mizutaka S, Tanizawa T. Robustness analysis of bimodal networks in the whole range of degree correlation. *Phys Rev E* (2016) 94(2-1):022308–7. doi:10.1103/PhysRevE.94.022308
56. Gan SL, Djauhari MA. New York stock exchange performance: Evidence from the forest of multidimensional minimum spanning trees. *J Stat Mech* (2015) 2015(12):P12005–23. doi:10.1088/1742-5468/2015/12/P12005
57. Nie CX, Song FT. Constructing financial network based on PMFG and threshold method. *Physica A: Stat Mech its Appl* (2018) 495:104–13. doi:10.1016/j.physa.2017.12.037
58. Hosseini SS, Wormald N, Tian TH. A weight-based information filtration algorithm for stock-correlation networks. *Physica A: Stat Mech its Appl* (2021) 563:125489–14. doi:10.1016/j.physa.2020.125489
59. Zhang DY, Broadstock DC. Global financial crisis and rising connectedness in the international commodity markets. *Int Rev Financ Anal* (2020) 68:101239–11. doi:10.1016/j.irfa.2018.08.003
60. Müller FM, Righi MB. Numerical comparison of multivariate models to forecasting risk measures. *Risk Manag* (2018) 20(1):29–50. doi:10.1057/s41283-017-0026-8
61. Liu XY, An HZ, Li HJ, Chen ZH, Feng SD, Wen SB. Features of spillover networks in international financial markets: Evidence from the G20 countries. *Physica A: Stat Mech its Appl* (2017) 479:265–78. doi:10.1016/j.physa.2017.03.016
62. Stavroglou SK, Pantelous AA, Stanley HE, Zuev KM. Hidden interactions in financial markets. *Proc Natl Acad Sci U S A* (2019) 116(22):10646–51. doi:10.1073/pnas.1819449116
63. Kim JM, Lee N, Hwang SY. A copula nonlinear granger causality. *Econ Model* (2020) 88:420–30. doi:10.1016/j.econmod.2019.09.052
64. Xu QF, Zhuo X, Jiang CX, Sun F, Huang X. Reverse restricted MIDAS model with application to US interest rate forecasts. *Commun Stat - Simulation Comput* (2021) 50(2):462–82. doi:10.1080/03610918.2018.1563148